

Increasing Trends of Guillain-Barré Syndrome (GBS) and Dengue in Hong Kong

Xiujuan Tang^{1,+}, Shi Zhao^{2,+}, Alice P.Y. Chiu^{2,*}, Xin Wang¹, Lin Yang³, and Daihai He^{2,*}

¹Shenzhen Center for Disease Control and Prevention, Shenzhen, China

²Department of Applied Mathematics, Hong Kong Polytechnic University, Hong Kong

³School of Nursing, Hong Kong Polytechnic University, Hong Kong

*daihai.he@polyu.edu.hk and alice.py.chiu@polyu.edu.hk

+these authors contributed equally to this work

ABSTRACT

Background

Guillain-Barré Syndrome (GBS) is a common type of severe acute paralytic neuropathy and associated with other virus infections such as dengue fever and Zika. This study investigate the relationship between GBS, dengue, local meteorological factors in Hong Kong and global climatic factors from January 2000 to June 2016.

Methods

The correlations between GBS, dengue, Multivariate El Niño Southern Oscillation Index (MEI) and local meteorological data were explored by the Spearman Rank correlations and cross-correlations between these time series. Poisson regression models were fitted to identify nonlinear associations between MEI and dengue. Cross wavelet analysis was applied to infer potential non-stationary oscillating associations among MEI, dengue and GBS.

Findings

An increasing trend was found for both GBS cases and imported dengue cases in Hong Kong. We found a weak but statistically significant negative correlation between GBS and local meteorological factors. MEI explained over 12% of dengue's variations from Poisson regression models. Wavelet analyses showed that there is possible non-stationary oscillating association between dengue and GBS from 2005 to 2015 in Hong Kong. Our study has led to an improved understanding of the timing and relationship between GBS, dengue and MEI.

Introduction

Guillain-Barré Syndrome (GBS) is the most common type of serious acute paralytic neuropathy, with approximately 100,000 new cases worldwide annually¹. Approximately two-thirds of these cases are believed to be triggered by prior infections². GBS has been associated with Zika virus³, Chikungunya fever and dengue fever¹. GBS cases show peaks in winters than in summers in Western countries⁴, but not in Latin America and Indian sub-continent⁴. Previous studies in Hong Kong did not identify any obvious seasonal patterns among adults or children GBS cases^{5,6}.

The multivariate El Niño Southern Oscillation index (MEI), is the most comprehensive global index to measure the intensity of El Niño Southern Oscillations (ENSO)⁷. MEI indicates warm events ("El Niño") from 2014 to present. Previous studies suggested the association between MEI and infectious disease transmission⁸.

Dengue virus (dengue) is of key public health significance because it can cause rapid and extensive epidemics and thus leads to stresses to the healthcare system⁹. Dengue has an estimated 50 million infections per year occurring in approximately 100 endemic countries, including many Southeast Asian countries¹⁰. The global spread of dengue is mainly driven by global trade, increasing travel, urban crowding and ineffective mosquito-control strategies¹¹, as well as temperature, rainfall and degree of urbanization¹².

Dengue is a flavivirus, where humans and mosquitoes are the only hosts¹¹. It is transmitted by *Aedes* mosquitoes infected with dengue viruses¹¹. While the principal vector *Aedes aegypti* is not found in Hong Kong, *Aedes albopictus* is

responsible for the local disease spread. In Hong Kong, over 90% of the dengue cases are imported cases, i.e. non-locally acquired¹³. dengue is mainly found in tropical and sub-tropical countries. They are endemic in many Southeast Asian countries and Southern China¹⁰. Previous studies by Tipayamongkholgul et al. and Hurtado-Diaz et al. used autoregressive models to examine the impact of El Nino on dengue incidence^{14,15}. A number of wavelet analyses studies had explored the non-stationary oscillating association between dengue and El Nino¹⁶⁻¹⁹. Van Panhuis et al. further reported that there are strong patterns of synchronous dengue transmission across eight Southeast Asian countries. Dengue cycles with a two to five-year periodicity were highly coherent with the Oceanic Nino Index. More synchrony was displayed with increasing temperature¹⁶. Cazelles et al. and Thai et al. also reported on a two to three-year periodicity between dengue and El Nino¹⁷. However, Johansson observed no association between them in Puerto Rico, Mexico and Thailand¹⁹.

In this work, we aim to study the trends of GBS and dengue in Hong Kong, the association between GBS, dengue and meteorological factors. Wavelet approaches are used to examine the non-stationary oscillating association among these factors.

Results

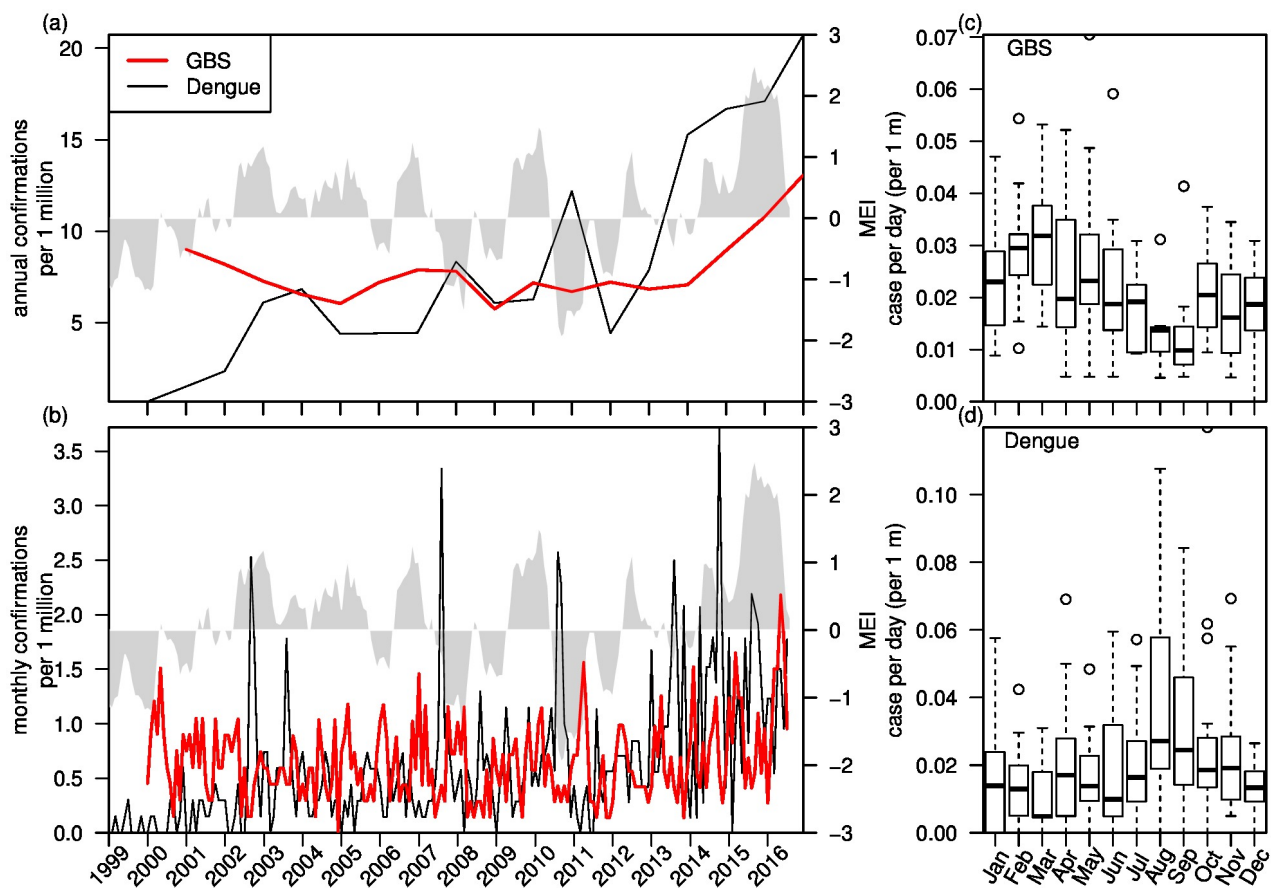


Figure 1. Trends and seasonality of GBS and dengue cases. (a) Annual cases of GBS and dengue cases show a sudden increase in recent years, MEI is represented by the shaded area. (b) Monthly cases of GBS and dengue cases, the shaded area is MEI. (c) Boxplot of GBS cases per day displays a seasonal pattern. (d) Boxplot of dengue cases per day also displays a seasonal pattern.

Figure 1 shows the trends and seasonality of GBS and dengue cases in Hong Kong. Annual GBS cases displays mild year-to-year fluctuations, but there is an evident increase after 2014 (Fig 1a). Annual dengue cases also display some variations, but it starts to rise sharply since 2012. Monthly cases of GBS shows mild spikes while monthly dengue cases shows some sharp spikes (Fig 1b). Fig 1c and 1d shows the boxplots of seasonal patterns of GBS and dengue. They display largely opposite seasonal patterns: GBS cases are low in August and September but are high in February and March (Fig 1c); dengue cases are low from February to April but are high in August and September (Fig 1d).

Historical data of MEI presents strong and statistically significant autocorrelations, which can be modelled by an Auto-regressive Model with a time lag of 2 months, i.e. an AR(2) model.

Correlations between GBS and Meteorological Factors

We first computed correlations between monthly GBS cases and monthly meteorological factors (i.e. median value of daily data in each month) from January 2000 to June 2016. We displayed the results in Table 1. We found weak but statistically significant correlations between mean temperature, minimum temperature, total evaporation with GBS cases. The strongest correlation was about -0.284. We conclude that lower temperature and less evaporation are correlated with more GBS cases in Hong Kong.

Table 1. Correlation (ρ) between monthly GBS cases and monthly meteorological factors from January 2000 to June 2016.

τ (months)	ρ	95%CI	adjusted p -value	signf
1	-0.029	(-0.167 , 0.111)	1.0000	
2	0.057	(-0.082 , 0.195)	1.0000	
3	0.009	(-0.130 , 0.148)	1.0000	
4	0.173	(0.035 , 0.305)	0.1713	
5	0.148	(0.009 , 0.281)	0.4407	
6	0.282	(0.149 , 0.406)	6.371e-04	***
7	0.292	(0.160 , 0.415)	3.353e-04	***
8	0.223	(0.087 , 0.352)	0.0182	*
9	0.109	(-0.031 , 0.244)	1.0000	
10	0.120	(-0.019 , 0.255)	1.0000	
11	0.093	(-0.047 , 0.229)	1.0000	
12	-0.015	(-0.154 , 0.125)	1.0000	

Mean pressure Maximum temperature Mean temperature Minimum temperature Mean dew point Mean relative humidity
 Mean amount of cloud Total bright sunshine Global solar radiation Total evaporation Prevailing wind direction

Cross-correlations of GBS and dengue

Hypothesizing that dengue could have an effect on GBS with a time lag of several months, we computed the cross-correlation between GBS and dengue cases with different time lags (Table 2). We found that dengue cases do not significantly correlate with GBS, unless a time lag is introduced. The cross-correlation coefficient attains a maximum at 0.2753 (95% CI: 0.1391, 0.4012) with a time lag of seven months. Our results suggest that dengue could have an effect on GBS with a time delay.

Cross-Correlations of dengue and GBS with MEI

We computed the cross correlations between dengue and MEI, and between GBS and MEI (Figure 2). The maximum cross-correlation is attained when there is a positive time lag of about three to five months in both GBS and dengue. Panel (a) shows that dengue is positively correlated with MEI, and the correlation is about 0.3 when the time lag is three months, which is biologically reasonable. However, panel (b) suggests that the cross-correlation between GBS and MEI is weaker (maximum correlation is about 0.2) than between dengue and MEI. These results are consistent with several studies that MEI played a crucial role on mosquito-borne diseases including dengue¹⁶⁻¹⁸, but possibly less related to GBS.

We found that dengue is significantly correlated with MEI for the period January 1999 to June 2016 when we did not consider time lag. The cross-correlation coefficient is 0.2048 (95%CI: 0.0694, 0.3328; p -value=0.003295).

Furthermore, we applied a Poisson regression model to estimate the association between dengue and MEI (eqn. 1), adopting a Moving Average (MA) model due to the relatively large oscillation of dengue data. The results of MA(3) and MA(5) models of dengue are reported in Fig. 3.

MEI coefficients (beta) and R^2 attain maximum when the lag are in between four to seven months (Figure 3). For both MA(3) and MA(5), the maximum R^2 are attained at lags 4 and lag 5, where they are greater than 0.11 (Appendix Table 3 and Table 4). Both results are consistent with previous studies^{14,15}.

Wavelet Analyses on MEI, dengue and GBS

In Figure 4(a), the wavelet transform suggest that MEI are significant at two to three-year periodic band. Figures 4(b) and 4(c) show that dengue and GBS display similar modes, both wavelet power spectrums are significant at around one-year periodic band.

Table 2. Cross-correlation (ρ) between GBS and dengue from January 2000 to June 2016. Time lag (τ , in months) indicates the number of months GBS lags behind dengue.

factor	ρ	95%CI	adjusted p -value	signif
mean.pressure	0.209	(0.072 , 0.338)	0.0336	*
temperature.max	-0.220	(-0.348 , -0.083)	0.0198	*
temperature.mean	-0.237	(-0.364 , -0.102)	0.0081	**
temperature.min	-0.244	(-0.371 , -0.109)	0.0056	**
mean.dew.point	-0.199	(-0.329 , -0.061)	0.0541	*
mean.relative.humidity	0.124	(-0.016 , 0.258)	0.8987	
mean.amount.of.cloud	0.139	(0.000 , 0.273)	0.5495	
total.bright.sunshine	-0.238	(-0.365 , -0.102)	0.0079	**
daily.global.solar.radiation	-0.188	(-0.319 , -0.050)	0.0853	*
total.evaporation	-0.284	(-0.407 , -0.151)	5.200e-04	***
prevailing.wind.direction	-0.176	(-0.308 , -0.038)	0.1413	

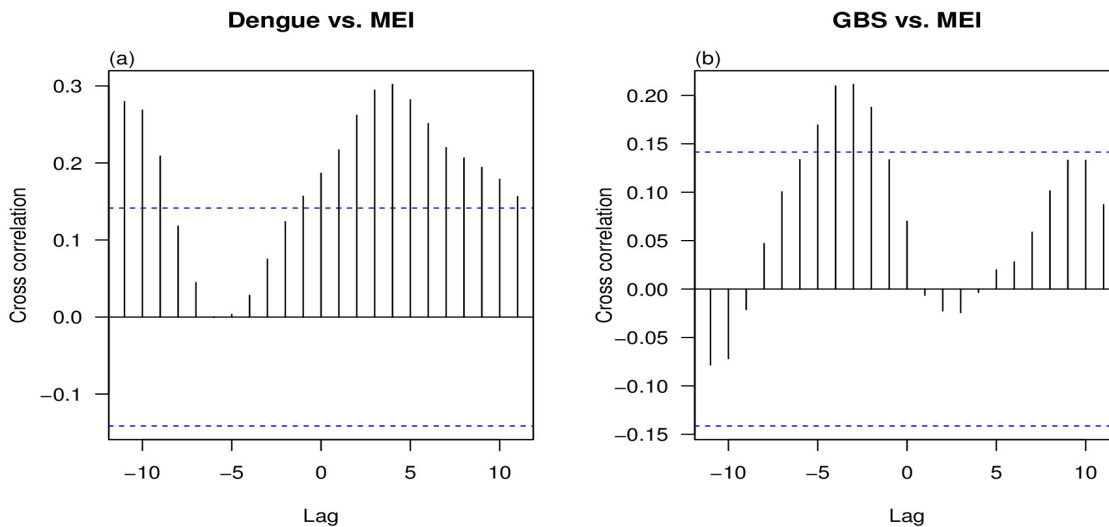


Figure 2. (a) Cross-correlation coefficient between dengue and MEI and (b) Cross-correlation coefficient between MEI and GBS. In both panels, we consider time lag of 0 to 11 months. Dashed lines on both panels indicate the significance level.

The cross wavelet analyses reveal considerable and significant coherence between MEI and both dengue and GBS since 2010, comparing with the situation before 2010 (see Fig. 5), which is similar with^{17,19}. The periods are at 1-2 years bond for MEI vs. dengue and 0.75-1.75 years bond for MEI vs. GBS from 2000-15.

Figure 6 suggests the oscillation mode (between dengue and GBS) is sometimes in a tone with a periodic bond of 0.5-1.5 years from 2000-15 in Hong Kong, the association became significant in the recent year. Interestingly, the appearance of the significant association between dengue and GBS seemingly coincided with major dengue outbreaks as shown in Fig. 6a-b.

Discussion

In this work, we reported increasing patterns of both GBS cases and imported dengue cases in Hong Kong, and investigated the possible mechanism behind said patterns. We found weak but statistically significant negative correlation between GBS and meteorological factors. Number of GBS cases was negatively correlated with both temperature and evaporation. Our findings are consistent with Webb et al's meta analyses that GBS cases were higher in winter than in summer⁴. The peak of dengue from 2013 to 2015 is largely consistent with that of MEI for the same period. MEI explained over 12% of dengue's variations from Poisson regression models. Our results are consistent with previous studies^{14,15}. Earlier clinical case studies reported dengue preceding GBS²⁰⁻²⁶. Our findings further showed that there is a cross-correlation between GBS and dengue cases. The increased magnitude of dengue outbreaks in Southern China could have played a role in the recent increases

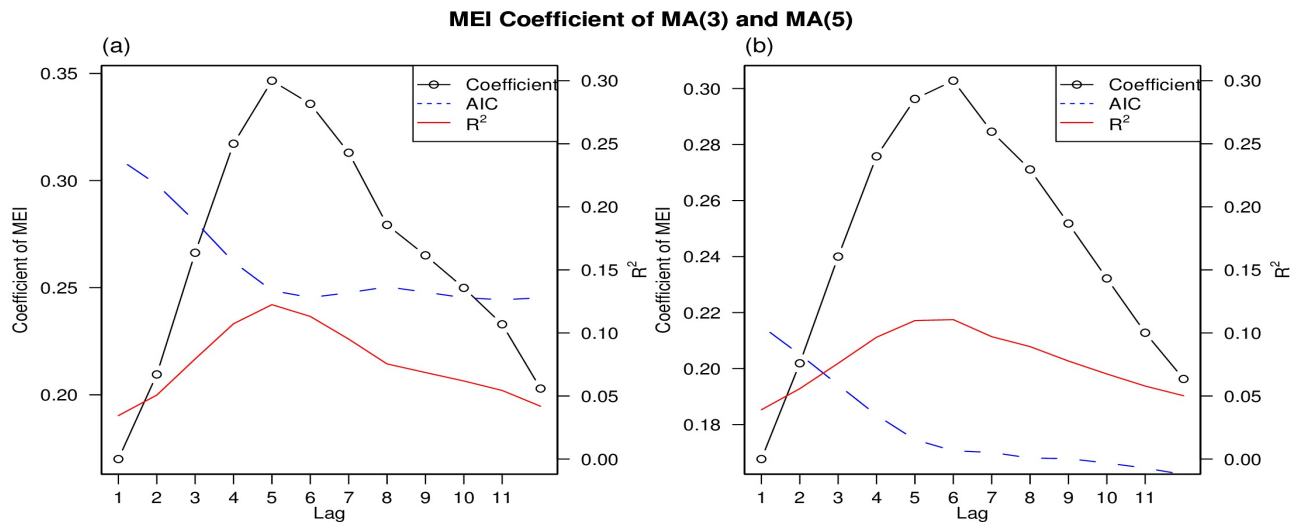


Figure 3. (a) MA(3) model of dengue (b) MA(5) model, displaying lags from 0 to 11 months. Black, dotted: Poisson regression coefficient of MEI (beta); red: R^2 ; blue, dashed: scaled AIC.

of GBS cases in Hong Kong. Our wavelet results showed that dengue and MEI oscillated in one to two-year periodic band. Our findings are consistent with earlier findings conducted in Vietnam, Thailand, and Southeast Asian countries in general^{16,17,27}. However, Johansson reported no association between dengue and multiyear climate variability on a study conducted in Mexico, Thailand and Puerto Rico¹⁹. As no ZIKV outbreaks had been reported in Hong Kong as of to date, local GBS cases are unlikely to be triggered by ZIKV. Thus, it is justifiable to use dengue and MEI data as an early warning for GBS surveillance. To our best knowledge, our study is the first to report on a possible non-stationary oscillation association between dengue and GBS. dengue reported cases displayed peaks in 2002, 2007, 2010 and 2014 respectively in Hong Kong, and phase plots of dengue and GBS indicated stronger coherency around those years. There are two major strengths in this study. First, although there had been several clinical case reports of dengue preceding GBS, we are novel to report on their association at the population level. Second, our wavelet analyses of GBS, dengue and MEI are well-suited to demonstrate the non-stationary oscillating association among them. This study is limited by several factors. First, GBS has both infectious and non-infectious triggers, and we do not have information about the antecedent events of reported GBS cases. Second, most of the dengue cases are imported cases, but we did not consider the population's travel patterns and the source country of infected cases. Third, dengue reported cases could be an underestimate of the true number of dengue infections in Hong Kong, since dengue could be a mild non-specific febrile illness that is difficult to distinguish from other illnesses. Our study has led to an improved understanding about the timing and relationship between MEI, GBS and dengue. Future studies should explore these disease patterns across a larger region scale to infer the mechanisms behind them. It would help to inform policymakers in designing appropriate prevention and control measures to combat these growing public health challenges.

Methods

Data and Methods

Epidemiological Data

Monthly GBS cases from January 2000 to June 2016 and dengue cases from January 1999 to June 2016 are downloaded from the website of Centre for Health Protection in Hong Kong (<http://www.chp.gov.hk>). An infected patient who recently travelled to a dengue endemic country is considered an imported dengue case, otherwise it is considered locally-acquired.

Meteorological Data

Meteorological data from January 1999 to June 2016 are downloaded from the website of Hong Kong Observatory (<http://www.hko.gov.hk>). After excluding missing data, we computed the median values of daily data in each month for further analyses. MEI data from January 1999 to June 2016 were downloaded from National Oceanic Atmospheric Administration's Earth System Research Laboratory (<http://www.esrl.noaa.gov/psd/enso/mei/>).

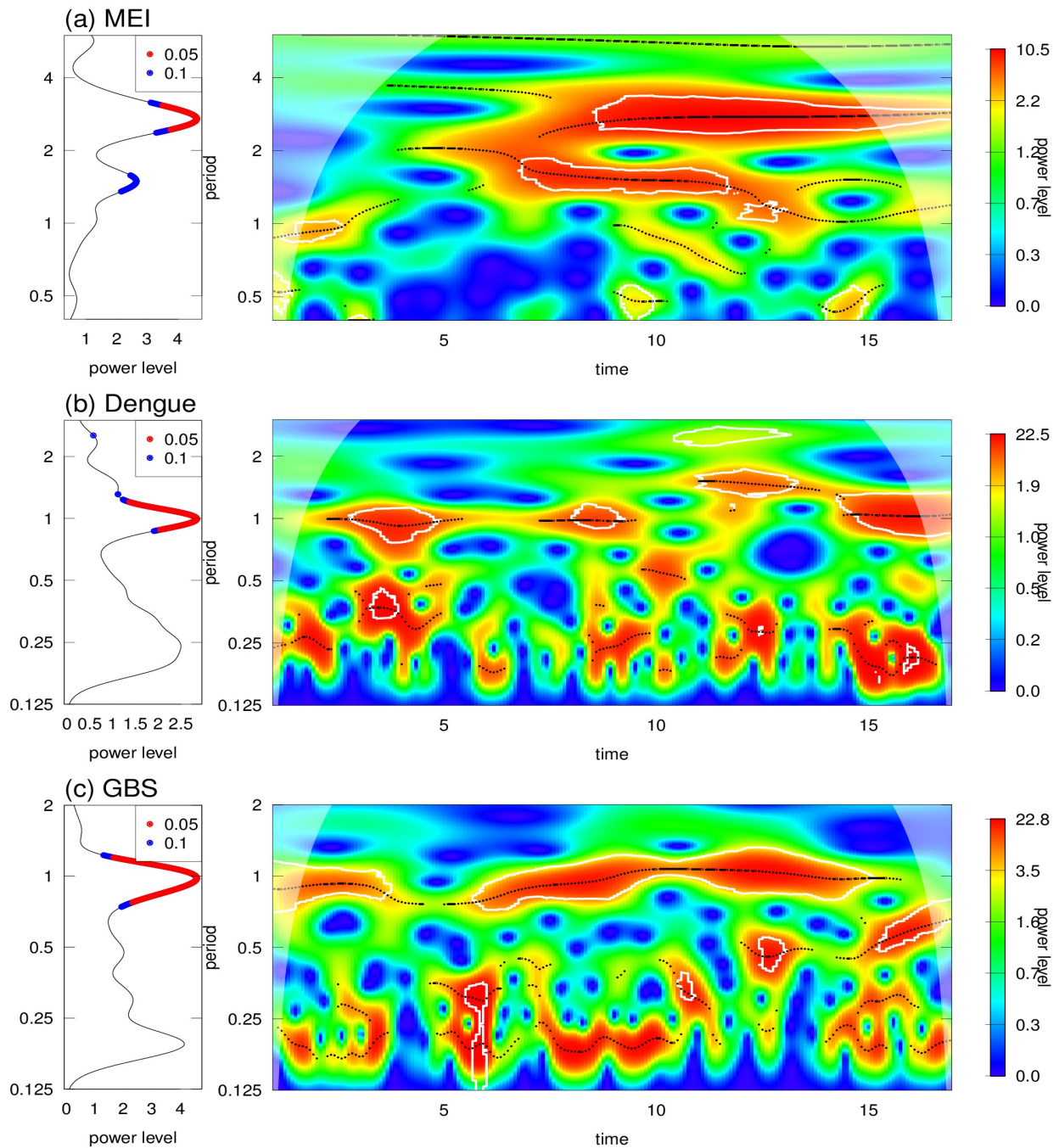


Figure 4. Wavelet analyses of MEI, dengue and GBS from 2000-2016 in panels (a), (b), and (c). Left panel: mean spectrum plots at 5% (blue) and 10% (red) thresholds. (ii) the right panel shows the wavelet power spectrum contour plots. The colour scheme is from blue to red, which represents increasing power level. The white line represents the 95% C.I. and the white shaded region is due to the edge effect. All data are transformed by taking square roots.

Statistical Analyses

We computed the Spearman's Rank Correlation between monthly GBS cases with the monthly median values of daily meteorological factors from January 2000 to June 2016 in Hong Kong. We then introduced time lags and computed the cross-correlation coefficient between monthly dengue cases and monthly GBS cases. We estimated the association between

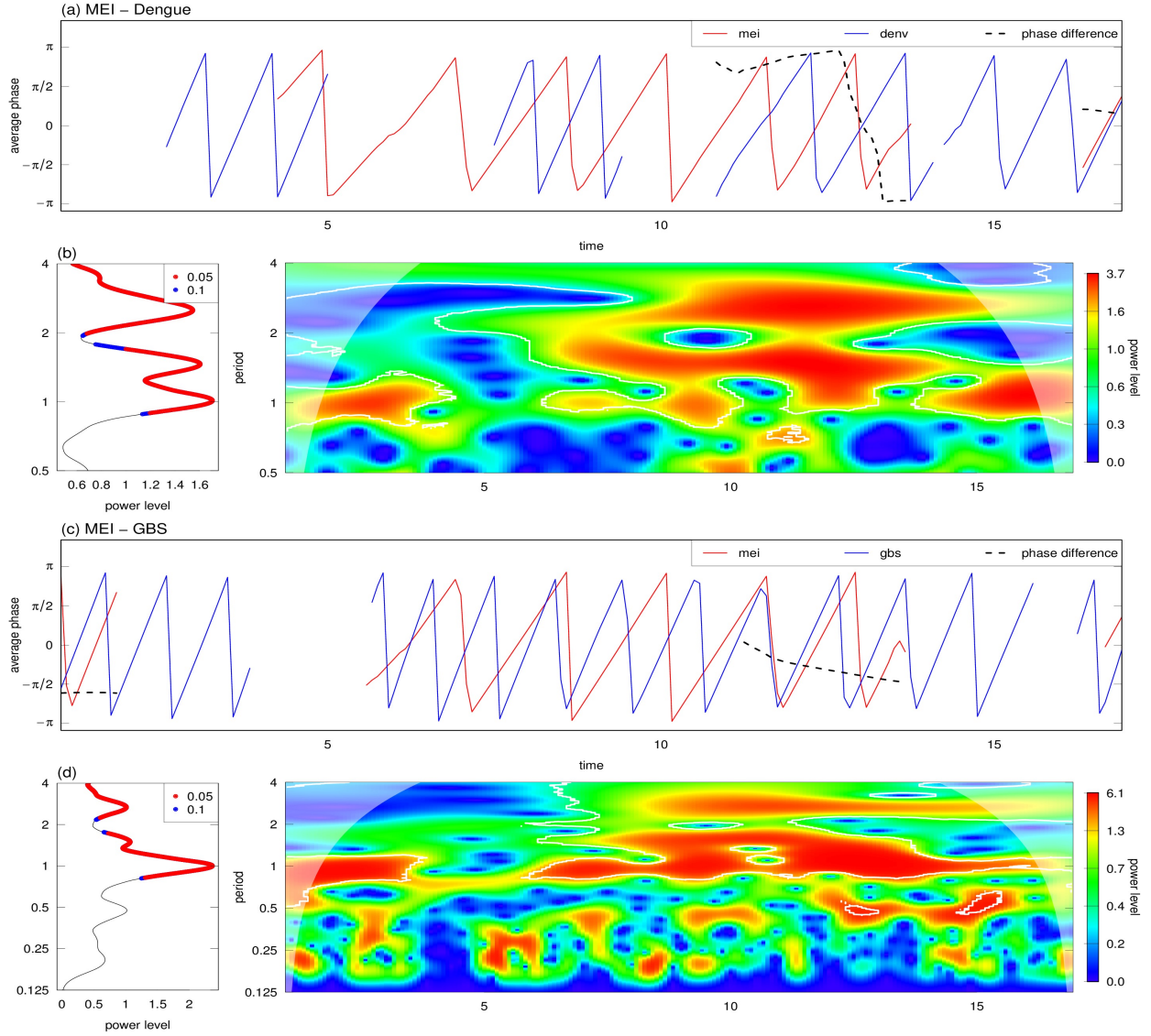


Figure 5. Wavelet coherence and phase plots among MEI, dengue, and GBS from 2000 to 2016. (a) and (c) show phase analyses. Data are shown in red and blue, and black dashed line shows phase difference. (b) and (d) show the cross-wavelet average power level and wavelet coherence plots, which share the same colour schemes as in Fig. 4. All data are transformed by taking square roots.

dengue and MEI by applying Poisson Regression model.

$$E[\text{dengue}_{t+\tau} | \text{MEI}_t] = \lambda_{\text{dengue}_{t+\tau}} = \exp(\alpha + \beta \text{MEI}_t + \varepsilon_{t+\tau}) \quad (1)$$

where where τ is the time lag with $\tau \in \{0, 1, \dots, 11\}$, λ is the Poisson parameter of dengue cases number at time $(t + \tau)$, α and β are the regression coefficients estimated by Maximum Likelihood approach and $\varepsilon_{t+\tau}$ is the error term. The absolute value of coefficient of MEI, $|\beta|$, can be interpreted as the non-linear association between MEI and dengue. The cross-correlation coefficients (ccf) are also used with different time lags.

Following previous works^{17–19}, we first transformed MEI, dengue and GBS data by taking square roots and then applied wavelet analyses to each set of these time series. Since MEI and the two diseases can be considered as “natural signal” such that the Morlet wavelet, $\psi(\cdot)$, could be applied as the “mother wavelet”:

$$\psi(t) = \pi^{-\frac{1}{4}} \exp[-i(2\pi f_0)t] \exp(-\frac{1}{2}t^2) \quad (2)$$

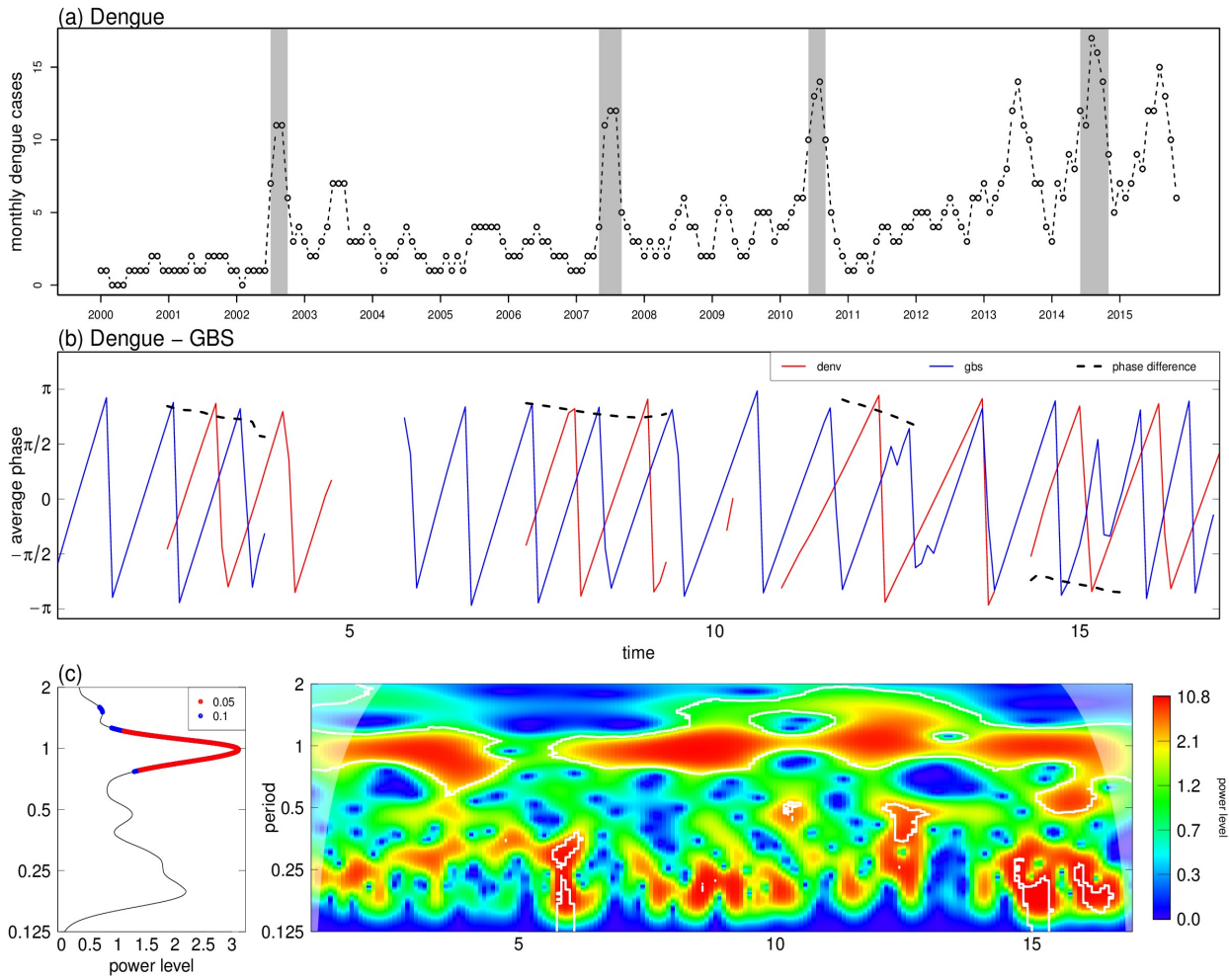


Figure 6. Wavelet coherence and phase plots of dengue vs. GBS data from 2000-15 in Hong Kong. Panel (a) is dengue time series with peaks shaded in grey. Panel (b) is phase plots of dengue vs. GBS, data are shown in red and blue, and black dashed line shows phase difference. Panel (c) show cross wavelet average power level and wavelet coherence plots of dengue vs. GBS, which share the same plot code as Fig. 4. The horizontal axis of 5, 10 and 15 represent year 2005, 2010 and 2015. All data are transformed by taking square roots.

where $(2\pi f_0)$ is the relative frequency of the sine function. The wavelet transformation of our data is:

$$W_{\psi,x}(a, \kappa) = \int_{-\infty}^{\infty} x(t) \bar{\psi}_{a,\kappa}^*(t) dt \quad (3)$$

where $W(\cdot)$ is the wavelet coefficient and it represents the contribution in transformation with (a, κ) given, a is the wavelet scale, and κ represent different time positions and $x(t)$ denotes the time series (i.e. MEI, dengue and GBS). $\bar{\psi}_{a,\kappa}^*(\cdot)$ is the complex conjugation of the reformed “mother wavelet”, ie, Morlet wavelet. We then applied the cross wavelet analysis to quantify the association among each dataset.

Statistical software R is used for all statistical analyses (version Ri386 3.3.1).

References

1. Willison, H.J., Jacobs, B.C. & van Doorn, P.A. Guillain-Barré syndrome. *Lancet*. **388**, 717-27; 10.1016/S0140-6736(16)00339-1 (2016).
2. Wakerley, B.R. & Yuki, N. Infectious and noninfectious triggers in Guillain-Barré syndrome. *Expert Rev Clin Immunol*. **9**, 627-39; 10.1586/1744666X.2013.811119 (2013).
3. Petterson, J.H., et al. How Did Zika Virus Emerge in the Pacific Islands and Latin America? *MBio*. **7**, pii: e01239-16; 10.1128/mBio.01239-16 (2016).
4. Webb, A.J., Brain, S.A., Wood, R., Rinaldi, S. & Turner, M.R. Seasonal variation in Guillain-Barré syndrome: a systematic review, meta-analysis and Oxfordshire cohort study. *J Neurol Neurosurg Psychiatry*. **86**, 1196-201; 10.1136/jnnp-2014-309056 (2015).
5. Hui, A.C., et al. Electrophysiological, clinical and epidemiological study of Guillain-Barré Syndrome in Hong Kong Chinese. *J Clin Neurosci*. **12**, 134-6 (2005).
6. Ma, Y.M., Liu, T.K. & Wong, V. Guillain-Barré syndrome in southern Chinese children: 32 year experience in Hong Kong. *Pediatr Int*. **52**, 13-9; 10.1111/j.1442-200X.2009.02951.x (2010).
7. Mazarella, A., Giuliacci, A. & Scafetta, N. Quantifying the Multivariate ENSO Index (MEI) coupling to CO₂ concentration and to the length of day variations. *Theor Appl Climatol*. **111**, 601-7 (2013).
8. Hay, S.I., et al. Etiology of interepidemic periods of mosquito-borne disease. *Proc Natl Acad Sci U S A*. **97**, 9335-9 (2000).
9. Shepard, D.S., Undurraga, E.A., Halasa, Y.A. & Stanaway, J.D. The global economic burden of dengue: a systematic analysis. *Lancet Infect Dis*. **16**, 935-41 (2016).
10. World Health Organization and the Special Programme for Research and Training in Tropical Diseases (TDR). Dengue guidelines for diagnosis, treatment, prevention and control: new edition. (WHO, 2009).
11. Simmons, C.P., Farrar, J.J., Nguyen, v.V. & Wills, B. Dengue. *N Engl J Med*. **366**, 1423-32; 10.1056/NEJMra1110265 (2012).
12. Bhatt, S., et al. The global distribution and burden of dengue. *Nature*. **496**, 504-7; 10.1038/nature12060 (2013).
13. Chuang, V., et al. Review of dengue fever cases in Hong Kong during 1998 to 2005. *Hong Kong Med J*. **14**, 170-7 (2008).
14. Tipayamongkolgul, M., Fang, C.T., Klinchan, S., Liu, C.M. & King, C.C. Effects of the El Niño-southern oscillation on dengue epidemics in Thailand, 1996-2005. *BMC Public Health*. **9**, 422; 10.1186/1471-2458-9-422 (2009).
15. Hurtado-Diaz, M., Riojas-Rodriguez, H., Rothenberg, S.J., Gomez-Dantes, H. & Cifuentes, E. Short communication: impact of climate variability on the incidence of dengue in Mexico. *Trop Med Int Health*. **12**, 1327-37 (2007).
16. van Panhuis, W.G., et al. Region-wide synchrony and traveling waves of dengue across eight countries in Southeast Asia. *Proc Natl Acad Sci U S A*. **112**, 13069-74; 10.1073/pnas.1501375112 (2015).
17. Cazelles, B., Chavez, M., McMichael, A.J. & Hales, S. Nonstationary influence of El Niño on the synchronous dengue epidemics in Thailand. *PLoS Med*. **2**, e106 (2005).
18. Thai, K.T., et al. Dengue dynamics in Binh Thuan province, southern Vietnam: periodicity, synchronicity and climate variability. *PLoS Negl Trop Dis*. **13**, e747; 10.1371/journal.pntd.0000747 (2010).
19. Johansson, M.A., Cummings, D.A. & Glass, G.E. Multiyear climate variability and dengue–El Niño southern oscillation, weather, and dengue incidence in Puerto Rico, Mexico, and Thailand: a longitudinal data analysis. *PLoS Med*. **6**, e1000168; 10.1371/journal.pmed.1000168 (2009).
20. Qureshi, N., Begum, A., Saha, P. & Hossain, M. Guillain-Barré syndrome following Dengue fever in adult patient. *Journal of Medicine*. **13**, 246-9 (2012).
21. Chen, T.Y. & Lee, C.T. Guillain-Barré syndrome following dengue fever. *Ann Emerg Med*. **50**, 94-5 (2007).
22. Kumar S & Prabhakar, S. Guillain-Barré syndrome occurring in the course of Dengue fever. *Neurology India*. **53**, 250 (2005).
23. Sulekha, C., Kumar, S. & Philip, J. Guillain-Barré syndrome following dengue fever. *Indian Pediatr*. **41**, 948-50 (2004).
24. Goncalves, E. Acute inflammatory demyelinating polyradiculoneuropathy (Guillain-Barré syndrome) following dengue fever. *Rev Inst Med Trop Sao Paulo*. **53**, 223-5 (2011).
25. Simon, O., et al. Early Guillain-Barré Syndrome associated with acute dengue fever. *J Clin Virol*. **77**, 29-31; 10.1016/j.jcv.2016.01.016 (2016).

26. Santos, N.Q., Azoubel, A.C., Lopes, A.A., Costa, G. & Bacellar, A. Guillain-Barré syndrome in the course of dengue: case report. *Arq Neuropsiquiatr.* **62**, 144-6 (2004).
27. Cuong, H.Q., et al. Quantifying the emergence of dengue in Hanoi, Vietnam: 1998-2009. *PLoS Negl Trop Dis.* **5**, e1322; 10.1371/journal.pntd.0001322 (2011).

Acknowledgements

This study was supported by ShenZhen Science and Technology Innovation Project Grant(JCYJ20150402102135501) and Start-up Fund for New Recruits from Hong Kong Polytechnic University.

Author contributions statement

TX, WX, ZS, CA and HD conceived the project. TX, ZS and HD analysed the results and wrote the draft. CA, YL and WX revised the article. All authors reviewed the manuscript.

Competing interests

The authors declare no competing financial interests.

Appendix

MEI Coefficient

MEI Coefficients, β , of MA(3) and MA(5) in Poisson Regression model (eqn. 1)

Table 3. MEI coefficient, β , list of Poisson Regression model with MEI taken 3 Moving Average (MA). Here, *** represents p -value under 0.0001, which is significant.

Lag τ	β of MEI	AIC	R^2	signif
0	0.1700	1058.90	0.0345	***
1	0.2095	1045.20	0.0507	***
2	0.2663	1025.60	0.0749	***
3	0.3172	1004.20	0.1073	***
4	0.3466	989.08	0.1224	***
5	0.3358	985.40	0.1131	***
6	0.3130	987.93	0.0951	***
7	0.2793	991.02	0.0754	***
8	0.2651	988.23	0.0868	***
9	0.2499	985.30	0.0619	***
10	0.2329	984.21	0.0544	***
11	0.2029	985.24	0.0419	***

Table 4. MEI coefficient, β , list of Poisson Regression model with MEI taken 5 Moving Average (MA). Here, *** represents p -value under 0.0001, which is significant.

Lag τ	β of MEI	AIC	R^2	signif
0	0.1677	970.35	0.0391	***
1	0.2019	955.28	0.0558	***
2	0.2400	939.18	0.0759	***
3	0.2758	923.19	0.0966	***
4	0.2963	910.24	0.1098	***
5	0.3028	904.36	0.1106	***
6	0.2846	903.50	0.0970	***
7	0.2711	900.54	0.0892	***
8	0.2518	900.22	0.0777	***
9	0.2322	897.89	0.0675	***
10	0.2128	895.24	0.0574	***
11	0.1963	891.83	0.0502	***